Heat transfer and pressure drop of perforated surface heat exchanger with passage enlargement and contraction

MASAO FUJII, YU SESHIMO and GORO YAMANAKA

Central Research Laboratory, Mitsubishi Electric Corporation,
1-1, Tsukaguchi-Honmachi 8-Chome, Amagasaki, Hyogo 661, Japan

Abstract—A new enhanced surface for forced-convection heat transfer effective in the range of Reynolds numbers lower than 3000 is proposed. The surface has many perforations and is bent to form a trapezoidal shape. A heat exchanger constructed with these surfaces has enlargement and contraction parts alternately along the flow passages. The mechanism of the heat transfer enhancement is studied experimentally by changing the surface geometries and heat exchanger configuration, and, in addition, by flow visualization. It is shown that the mechanism of the heat transfer enhancement is due to the secondary flow induced by the suction and injection through the perforations, and to the frequent boundary layer interruptions at each contraction part. Dimensionless correlations on the heat transfer and pressure drop are presented.

1. INTRODUCTION

TWO OF the most conventional extended surface heat exchangers are the plate-fin and the tube-fin types, which are widely used in air conditioners, automobiles and electronic equipment.

Recently, the heat exchangers have been required to be much more compact in size and lighter in weight because of restrictions in setup space and for economical reasons. Furthermore, low frontal velocities are required in order to reduce the noise level of the exchangers. As more compact heat exchangers are developed, the smaller the hydraulic diameter becomes, by using more closely spaced fins, and with low velocities the design Reynolds number also becomes smaller. It is therefore necessary to develop an enhancement technique in forced-convection heat transfer at low Reynolds numbers in order to achieve high performance of compact heat exchangers. In this paper, a new enhancement technique in forced-convection heat transfer in the range of Reynolds numbers lower than 3000 is presented.

An excellent source of design information on the compact heat exchanger surface is a monograph by Kays and London published in 1964 [1] and in 1984 [2], and most of the developed surfaces [3] in use until now are more or less related to that monograph. According to the monograph, the surfaces efficient in industrial heat exchangers in the range of low Reynolds numbers are interrupted fins such as strip and louver fins. The interrupted fins have boundary layers that develop anew after each interruption, and thus exhibit higher heat transfer coefficients than those of plain fins.

However, there have been no other advanced concepts on enhancement techniques at low Reynolds numbers (except these interrupted fins) since Kays and London.

The present authors have proposed an advanced concept on the enhancement technique in forced-convection heat transfer and also on the performance of an advanced surface [4]. The surface had many perforations and was bent to form a trapezoidal shape. The phase of each adjacent surface was shifted by a half-pitch, and therefore a heat exchanger constructed with these surfaces had enlargement and contraction parts alternately along the flow passage, as shown in Fig. 1. The heat transfer coefficient of the heat exchanger at the same Reynolds number was about three times that of a similar heat exchanger with plain surfaces, and also about 2.2 times at the same pumping power. Furthermore, it was judged that the mechanism of the heat transfer enhancement would be due to the secondary flow through perforations and also due to the boundary layer interruption, which means that the boundary layer was developing anew at each contraction.

In the present paper, the mechanism of the heat transfer enhancement of the advanced heat exchanger was studied experimentally by changing the surface geometries and heat exchanger configuration, and, in addition, by flow visualization.

2. EXPERIMENTAL APPARATUS AND PROCEDURE

The heat transfer measurements were carried out using a transient test technique, as shown in refs. [4, 5]. The test heat exchanger constructed with heating surfaces was set in an open circuit wind tunnel. The heating surfaces were made of stainless steel, 0.5 mm thick. Twenty such heating surfaces were piled up with

NOMENCLATURE

d	diameter of perforation	S	width between surfaces
De	hydraulic diameter (S_1+S_2)	u	mean velocity of main flow, $(u_1+u_2)/2$
f	mean drag coefficient which includes both skin friction and form drag over the surface, defined by equation (3)	v	mean velocity of secondary flow.
h	heat transfer coefficient		Greek symbols
K	dimensionless factor, defined by equation (5)	α	ratio of cross-sectional area of contraction part to that of enlargement part, defined by equation (6)
L	total length of heat exchanger surface	β	porosity of heat transfer surface
l	length of a flat part	λ	thermal conductivity of fluid
Nu	Nusselt number, defined by equation (1)	v	kinematic viscosity of fluid
ΔP	pressure drop through heat exchanger	ρ	density of fluid.
ΔP_d	static pressure difference, defined by equation (4)		Subscripts
q	flow rate per unit area	1	enlargement part
Re	Reynolds number, defined by equation (2)	2	contraction part.

a spacing of 5.5 mm to compose a heat exchanger with 120×120 mm^2 cross-sectional area.

Table 1 gives the dimensions of the test heat exchangers. Figure 2 shows a schematic diagram of those heat exchangers. The perforations were in a staggered array, with diameter d and with a constant pitch corresponding to their porosity β. The heat exchangers from (P-3) to (P-11) are of the same shape as (P-2).

The air flow rate in the wind tunnel was kept constant at a predetermined value. The air was heated with an electric resistance heating screen up to about 10°C above the ambient temperature. The heating was continued until the heat exchanger reached a uniform temperature, which was confirmed from a negligible difference between the air temperatures at the inlet and outlet. The air temperature was measured with a thermopile made by 16 copper–constantan thermo-
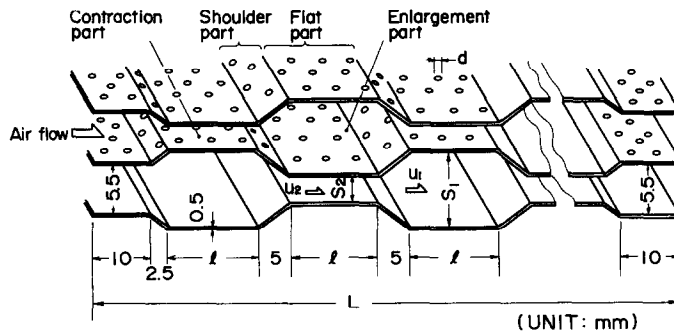

FIG. 1. Schematic diagram of advanced heat exchanger configuration.

Table 1. Test heat exchangers

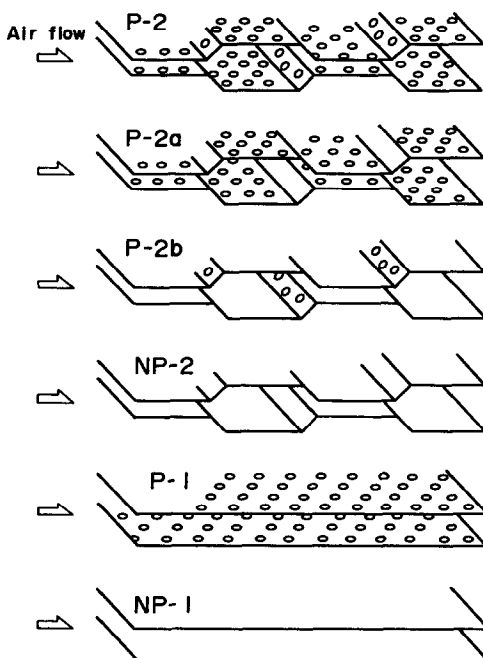| No.	S_1 (mm)	S_2 (mm)	l (mm)	L (mm)	d (mm)	β	α
P-1	5.5	5.5	–	100.0			1.00
P-2			15.0				
P-3	8.6	2.4		52.3			0.28
P-4			7.5	92.4		0.145	
P-5	8.3	2.7		132.4	2.0		0.33
P-6	7.6	3.4					0.45
P-7			15.0	100.0			
P-8	9.5	1.5				0.296	0.16
P-9						0.086	
P-10	8.9	2.1	20.0	111.1	4.0	0.145	0.24
P-11			15.0	100.0			
NP-1	5.5	5.5	–	100.0	–	–	1.00
NP-2	8.6	2.4	15.0				0.28

FIG. 2. Schematic diagram of test heat exchangers.

couples, each 0.1 mm in diameter. After the stable condition was reached, the power to the heating screen was turned off. The temperature–time history of the outlet air was continuously recorded. This temperature–time history of the air depended on the heat transfer rate from the heat exchanger, and the heat transfer coefficient was determined by a direct curve matching method.

The average of the initial and final outlet air temperatures was used in the data reduction.

The pressure drop ΔP through the heat exchanger was obtained by measuring the difference in the wall static pressure difference.

The experimental results of the heat transfer and pressure drop of a parallel plate heat exchanger (NP-1), shown in Fig. 2, were compared with the data obtained by other investigators [6, 7], and were almost in agreement [4]. Therefore, the transient test technique employed in this study was confirmed to be reliable.

In this study, a flow of water was visualized mixing aluminum powder as the tracer for a model five times as large as the actual heat exchanger.

3. RESULTS AND DISCUSSION

The heat transfer and pressure drop characteristics of the heat exchanger were presented in terms of the following nondimensional groups:

$$Nu = h \cdot De / \lambda \qquad (1)$$

$$Re = u \cdot De / v \qquad (2)$$

$$f = \Delta P \left(\frac{4L}{De} \cdot \frac{\rho u^2}{2} \right)^{-1}. \qquad (3)$$

The heat transfer coefficient was obtained by considering the porosity of the heating surface.

3.1. Flow observation

The flow of water with aluminum powder in the advanced heat exchanger was observed by using a model five times as large as the actual test heat exchanger (P-2).

The aspect of the flow is shown in Fig. 3. Figure 4 shows the flow in the contraction part for three different Reynolds numbers. The sketch is illustrated in Fig. 5.

The results of the observation are summarized in the following.

Contraction part. (1) Judging from the fact that the aluminum powder in the water flew regularly and smoothly in the contraction part, the flow developing from each entrance of the contraction part seemed to form a laminar boundary layer. Thus the heat transfer in this region was enhanced possibly by the effect of the boundary layer interruption.

(2) Fluid injection through perforations was observed. The injected flow joined the main flow without disturbing it, as shown in Figs. 4(a) and (b), but the injected flow through perforations caused the boundary layer to become locally turbulent. With the increase of the Reynolds number, as shown in Fig. 4(c), the main flow was gradually disturbed by the injected flow. The fluid injection from perforations might have increased the enthalpy transport by removing the superheated boundary layer, and accelerating the fluid flow in the boundary layer. Thus, it might be thought that the fluid injection improved the heat transfer.

(3) The injection velocity was larger at the rear part of the contraction part. This fact suggests that the static pressure difference between the contraction part and the adjacent enlargement part is changing along the flow passage.

Enlargement part. (4) Fluid suction through perforations was observed, and thus the main flow was brought close to the surface. The fluid suction could make the boundary layers thinner and thereby augmented the heat transfer.

(5) At the entrance of each enlargement part, the main flow was separated to generate many vortices. Thus the fluid flow became turbulent, resulting in the turbulent heat transfer in the enlargement part.

(6) The fluid injection and suction were remarkable through the perforations at each shoulder part shown in Fig. 1.

As stated in (2) and (4), the injection and suction through the perforated surfaces were achieved simultaneously in this heat exchanger. The present authors would like to call this injection and suction phenomena the 'breathing effect', which means the perforated surfaces breathe through the perforations.

3.2. Effect of heat exchanger configuration

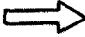Results for the heat exchangers shown in Fig. 2 are shown in Fig. 6. The heat exchangers (P-2a) and (P-

FIG. 3. Aspect of water flow in advanced heat exchanger ($Re = 400$).

2b) were made by closing some part of the perforations of the heat exchanger (P-2) with very thin adhesive tapes, of which the thermal resistance and the heat capacity were so small as to be negligible compared with those of the heat exchanger surfaces.

The parallel plate heat exchangers (NP-1) and (P-1) had almost the same performance, and thus it seemed that the perforations had no effect at all on the performance of the parallel plate heat exchanger within this experimental range of the Reynolds number, as stated in ref. [4] and also shown by Liang [8].

The heat exchanger (NP-2) without perforations showed an increase in both Nu and f compared with the parallel plate heat exchanger (NP-1). It is considered that the enhancement of heat transfer of the heat exchanger (NP-2) was due to the effect of the boundary layer interruption in the contraction parts, and the flow separation and reattachment in the enlargement parts. However, the effect of the turbulent flow in the enlargement part on the enhancement of heat transfer might be small, because the flow velocity in the enlargement part was smaller than that in the contraction part. This could be confirmed by the fact that the dependence of Nu on Re of the heat exchanger (NP-2) was similar to that of the parallel plate heat exchanger (NP-1). Thus the increase in f of the heat exchanger (NP-2) might be mainly due to the increase in the skin friction in the contraction parts. The form drag at each contraction and enlargement part also made the pressure drop increase, but its effect might be small compared with the skin friction, because the enlargement and contraction were not abrupt.

The heat exchanger (P-2b), which had perforations only on the shoulder parts of the heat exchanger (NP-2), had the same heat transfer characteristics as the heat exchanger (NP-2). However, the pressure drop of the heat exchanger (P-2b) was much smaller when compared with that of the heat exchanger (NP-2). The magnitude was almost the same with the heat exchanger (P-2) which had perforations uniformly distributed on the heating surface. Hence, the perforations at the shoulder part were considered to contribute to the decrease in pressure drop.

The Nusselt numbers of the heat exchanger (P-2a), which had perforations only on the flat parts of the heat exchanger (NP-2), were much larger when compared with those of the heat exchanger (NP-2), and were almost the same as those of the heat exchanger (P-2). The pressure drop of the heat exchanger (P-2a) was almost the same as that of the heat exchanger (NP-2).

In the case when there are no perforations at the shoulder parts, the entrance region of the enlargement part may almost be a dead zone for the heat transfer because of the flow separation. The flow separation causes the increase in form drag. However, in the case when there are perforations at the shoulder parts, such as in the heat exchangers (P-2) and (P-2b), the fluid flow is injected into the dead zone so that the heat transfer characteristics can be improved and the form drag is reduced. At the same time, since the main flow is separated by the perforations at the shoulder parts, the flow velocity in the contraction part becomes small, resulting in the decrease of the heat transfer coefficient and friction loss. Consequently, the perforations at the shoulder parts do not affect the heat transfer, but do the pressure drop.

In general, the perforations at the shoulder parts contribute to the decrease in pressure drop, and the perforations at the flat parts contribute to the enhancement in heat transfer caused by the breathing effect. Such a speculation leads to the conclusion that the heat transfer surfaces of (P-2) type are most appropriate for the advanced heat exchanger.

### 3.3. *Effect of surface geometry*

Based on the experimental results and flow visualization, a simple model is set up to clarify the effect of the surface geometry on the performance of the advanced heat exchanger, assuming the steady flow of an ideal fluid.

In Fig. 1, the static pressure difference ΔP_d between the contraction part and the adjacent enlargement part is given by Bernoulli's theory as follows:
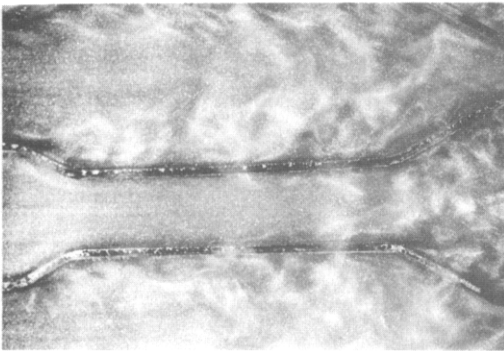
$$\Delta P_d = \frac{\rho}{2}(u_2^2 - u_1^2). \qquad (4)$$
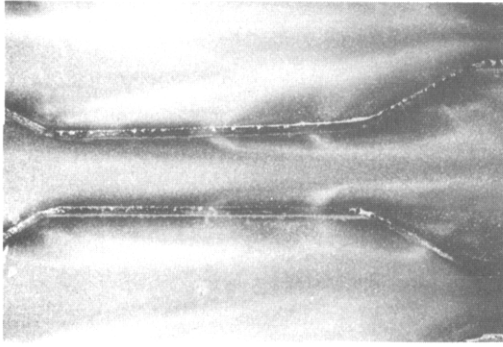
(a)
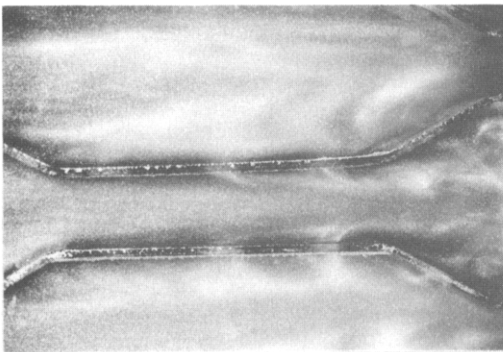
(b)

(c)

FIG. 4. Flow in the contraction part for three different Reynolds numbers: (a) $Re = 400$; (b) $Re = 600$; (c) $Re = 2000$.

It can be considered that this pressure difference acts as a driving force of the secondary flow through the perforations. Here, it is assumed that the flow rate through the perforations is very small, and thus it does not influence the velocities u_1 and u_2.

Assuming that the injection (or suction) velocity v is uniform and constant all over the perforated surface
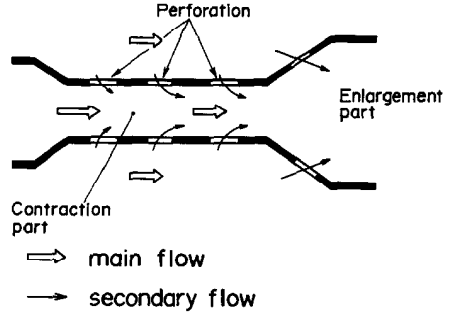
$$\Delta P_d = K\frac{\rho}{2}v^2. \qquad (5)$$

FIG. 5. Sketch of a flow in contraction part.

The dimensionless factor K depends on the porosity β. K decreases with an increase in β. β is a function of the diameter and pitch of perforations.

If the injection (or suction) velocity v is negligibly small, the law of the conservation of mass yields

$$u_1/u_2 = S_2/S_1 = \alpha(<1). \qquad (6)$$

The flow rate through the perforations per unit area of the heat exchanger surface is then

$$q = \frac{2\rho u\beta}{1+\alpha}\sqrt{\left(\frac{1-\alpha^2}{K}\right)}. \qquad (7)$$

Equation (7) indicates that the flow rate through the perforations increases with the increase of β and the decrease of α since the derivative of q by α is negative. The increase in flow rate through the perforations, that is, the increase in the breathing effect, leads to the augmentation of the heat transfer.

The increase in β at the shoulder part brings about the decrease of the pressure drop as mentioned in
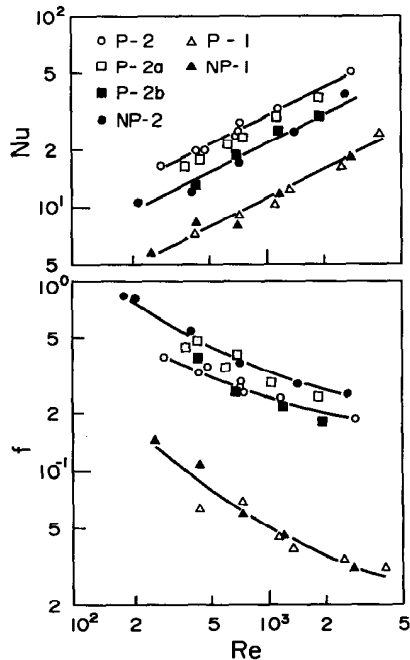

FIG. 6. Effect of heat exchanger configuration on heat transfer and pressure drop characteristics.

Section 3.2, and the decrease in α can increase the pressure drop because of the increase in the skin friction in the contraction part and also the increase in the form drag at each contraction and enlargement part.

Length l is also one of the main factors influencing the performance of the advanced heat exchanger. As length l decreases, the heat transfer rate will increase because of the frequent boundary layer interruption at each contraction part as stated in the summary of the result of the flow observation (1). Also the pressure drop will increase because of the frequent boundary layer interruption and the increase in number of contraction and enlargement parts.

Thus, it can be predicted that the performance of the heat exchanger will be mainly dominated by the geometrical factors such as α, β and l.

3.3.1. *Effect of* α. Figure 7 shows the experimental results indicating the effect of α. As the ratio of the cross-sectional area α decreases, both the Nusselt number and the drag coefficient increases.

3.3.2. *Effect of* β. Figure 8 shows the experimental results indicating the effect of β. As β increases, the heat transfer characteristics are improved a little, and the drag coefficient decreases dramatically.

Figure 9 shows the effect of the diameter of the perforation d on the performance of the heat exchanger at the same β (= 0.145). With the decrease in the perforation diameter, the Nusselt number seems to increase slightly. However, the effect of the perforation diameter on the performance of the heat exchanger is relatively small at the same β,
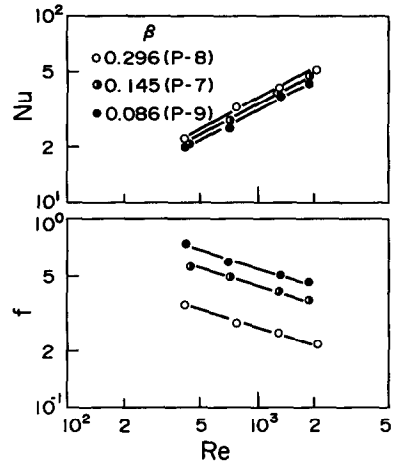

FIG. 8. Effect of porosity, β.

and thus the effect of the perforation diameter can be ignored in practical application.

3.3.3. *Effect of* l. Figure 10 shows the effect of l on the performance of the heat exchanger. As the length l decreases, the heat transfer is enhanced and the drag coefficient increases.

Figure 11 shows the effect of the total length L on the performance quoted in ref. [4]. From Figs. 10 and 11, it is known that the heat transfer and pressure drop of the heat exchanger is not dominated by the length L, but by the length l.

The experimental results shown in Figs. 7, 8 and 10 indicate that the prediction is almost correct.

4. CORRELATION FOR ADVANCED HEAT EXCHANGER

In the preceding section, the effects of the surface geometries on the heat transfer and pressure drop characteristics of the advanced heat exchanger were,
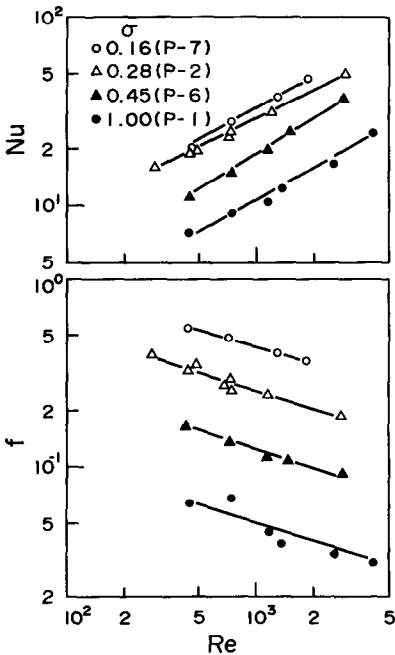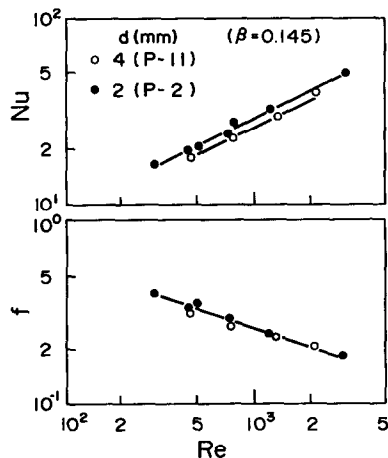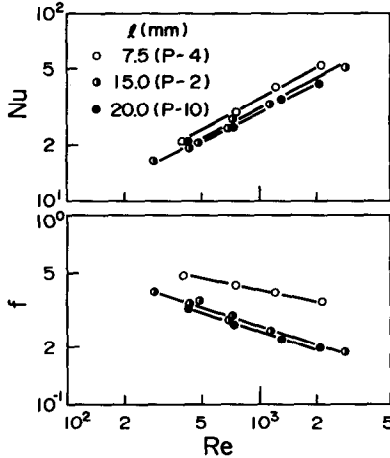

FIG. 7. Effect of α.

FIG. 9. Effect of perforation diameter, d.

Fig. 10. Effect of contraction length, l.

to some extent, clarified. Although the mechanism of the heat transfer on the heat exchanger surface was not fully understood, the authors attempted to establish the dimensionless correlation of the heat transfer coefficient and the drag coefficient for practical application.
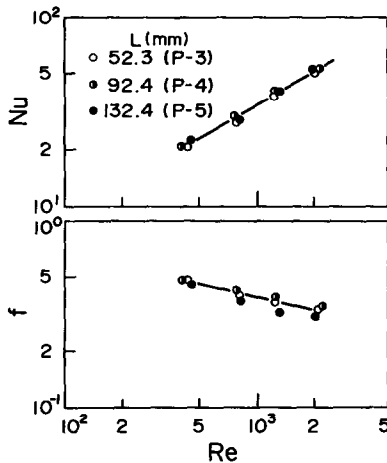
The results were as follows:

$$Nu = 1.04Re^{0.55}(1-\alpha^2)^{2.4}\beta^{0.08}(De/l)^{0.21} \quad (8)$$

$$f = 0.20Re^{-0.34}\alpha^{-1.23}\beta^{-0.6}(De/l)^{0.69} \quad (9)$$

where $0.16 \leqslant \alpha \leqslant 0.45$, $0.086 \leqslant \beta \leqslant 0.296$, $250 \leqslant Re \leqslant 3000$.

The experimental data were well correlated by equations (8) and (9) within the uncertainty of $\pm 15\%$ for Nu and $\pm 20\%$ for f.

Fig. 11. Effect of total length, L.

5. CONCLUSIONS

From the result of the flow visualization, the breathing effect, which was the phenomenon that the fluid was injected and sucked through the perforated surface, was observed. At each contraction part, the boundary layer was developed and at each enlargement part, the turbulent flow was dominant. Thus, it was certain that the heat transfer enhancement of the advanced heat exchanger was attributed to the secondary flow caused by the breathing effect and the frequent boundary layer interruptions at each contraction part.

The mechanism of the heat transfer enhancement of the advanced heat exchanger was studied experimentally for different surface geometries and heat exchanger configuration (α, β, l). As β increased and α decreased, which meant that the injection (or suction) flow rate through the perforated surface increased, the heat transfer characteristics were improved. Furthermore, the heat transfer characteristics were improved with the decrease in l. Thus, the mechanism of the heat transfer enhancement for the advanced heat exchanger coincided with the prediction obtained from the results of the flow visualization.

Finally, the dimensionless correlations (8) and (9) on the Nusselt number and the drag coefficient were presented. These correlations will be very useful for the optimum design of compact heat exchangers.

REFERENCES

1. W. M. Kays and A. L. London, Compact Heat Exchangers. McGraw-Hill, New York (1964).
2. W. M. Kays and A. L. London, Compact Heat Exchangers. McGraw-Hill, New York (1984).
3. R. K. Shah, Classification of heat exchangers. In Heat Exchangers, p. 9. McGraw-Hill, New York (1981).
4. Y. Seshimo, M. Fujii and G. Yamanaka, An experimental study on performance of perforated duct with enlargement and contraction (1st report, An evaluation for a heating surface), 23rd National Heat Transfer Symposium of Japan, p. 346 (1986) (in Japanese).
5. R. K. Shah, Compact heat exchangers. In Heat Exchangers, p. 111. McGraw-Hill, New York (1981).
6. K. Marumoto, Y. Seshimo and G. Yamanaka, A study of wetted surface humidifier ((1) humidification characteristics), Preprint of Joint Conf. between Soc. of Heating, Air-conditioning and Sanitary Engineers of Japan and Japanese Association of Refrigeration, p. 89 (1986) (in Japanese).
7. R. K. Shah and A. L. London, Laminar flow forced convection in ducts. In Advances in Heat Transfer. Academic Press, New York (1978).
8. C. Y. Liang, Heat Transfer, flow friction noise and vibration studies of perforated surfaces. Ph.D. Thesis, Dept. of Mechanical Engineering, Univ. of Michigan (1975).

TRANSFERT DE CHALEUR ET PERTE DE CHARGE D'ECHANGEUR DE CHALEUR A PLAQUES PERFOREES AVEC ELARGISSEMENT ET CONTRACTION DE PASSAGE

Résumé—On propose une surface nouvelle pour le transfert thermique efficace de convection forcée, dans le domaine des nombres de Reynolds inférieurs à 3000. La surface a de nombreuses perforations et elle a une forme trapézoïdale. Un échangeur construit avec ces surfaces présente des élargissements et des contractions alternées le long de l'écoulement. On étudie expérimentalement le mécanisme de l'accroissement du transfert thermique en changeant les géométries de surface et la configuration de l'échangeur, et de plus par visualisation de l'écoulement. On montre que le mécanisme de l'accroissement de transfert est dû à l'écoulement secondaire induit par succion et injection à travers les perforations, et aux interruptions fréquentes des couches limites à chaque contraction. Des formules adimensionnelles sont présentées pour le transfert de chaleur et la perte de charge.

WÄRMEÜBERGANG UND DRUCKVERLUST IN WÄRMEÜBERTRAGERN MIT PERFORIERTEN OBERFLÄCHEN SOWIE ERWEITERUNGEN UND VERENGUNGEN DES STRÖMUNGSKANALS

Zusammenfassung—Es wird eine verbesserte Übertragungsfläche für den Wärmeübergang bei erzwungener Konvektion vorgeschlagen, die im Bereich von Reynolds-Zahlen kleiner als 3000 wirksam ist. Die Oberfläche ist stark perforiert und trapezförmig gebogen. Ein aus diesen Flächen konstruierter Wärmeübertrager weist entlang den Strömungskanälen wechselweise Erweiterungen und Verengungen auf. Die Verbesserung des Wärmeübergangs wird experimentell untersucht durch Variation der Oberflächengeometrie und der Wärmeübertragerkonfiguration und zusätzlich durch Sichtbarmachung der Strömung. Es wird gezeigt, daß die Verbesserung des Wärmeübergangs auf die Sekundärströmung zurückzuführen ist, die durch Ansaugung und Injektion durch die Perforation erzeugt wird, und auf die häufig auftretenden Grenzschichtunterbrechungen an jeder Verengung. Es werden dimensionslose Korrelationen für Wärmeübergang und Druckverlust vorgestellt.

ТЕПЛООБМЕН И ПАДЕНИЕ ДАВЛЕНИЯ В ТЕПЛООБМЕННИКЕ С ПЕРФОРИРОВАННЫМИ ПОВЕРХНОСТЯМИ И КАНАЛАМИ ПЕРЕМЕННОГО СЕЧЕНИЯ

Аннотация—Предложена новая поверхность для интенсификации теплообмена вынужденной конвекцией в диапазоне значений числа Рейнольдса ниже 3000. На поверхности имеется множество отверстий и, кроме того, она изогнута в форме трапеции. Теплообменник с такой поверхностью конструктивно состоит из участков переменного сечения, расположенных вдоль потока. Механизм интенсификации теплообмена исследуется эбспериментально путем изменения геометрии поверхностей и формы теплообменника, а также путем визуализации течения. Показано, что интенсификация теплообмена происходит за счет вторичного течения, вызываемого отсосом и вдувом через отверстия, а также за счет частых разрывов пограничного слоя в сужающихся частях каналов. Представлены безразмерные обобщенные соотношения для расчета теплообмена и перепада давления.